Supplementary Information for "Finite-size correction for slab supercell calculations of materials with spontaneous polarization"

Su-Hyun Yoo,[1,*] Mira Todorova,[1,†] Darshana Wickramaratne,[2,3]
Leigh Weston,[2] Chris G. Van de Walle,[2] and Jörg Neugebauer[1]

[1] *Department of Computational Materials Design, Max-Planck-Institut für Eisenforschung GmbH, Max-Planck-Str. 1, D-40237 Düsseldorf, Germany*

[2] *Materials Department, University of California Santa Barbara, USA*

[3] *Center for Computational Materials Science, US Naval Research Laboratory, Washington DC 20375, USA*

(Dated: March 25, 2021)

* yoo@mpie.de

† m.todorova@mpie.de

I. SUPPLEMENTARY NOTES

A. Additional comments about the definition of the polarization charge q_{P}

In the main text we defined q_{P} as the difference between the formal polarization of the wurtzite (WZ) and the zinc-blende (ZB) phases:

$$q_{\mathrm{P}} = P_{\mathrm{f}}^{\mathrm{WZ}} - P_{\mathrm{f}}^{\mathrm{ZB}} = P_{\mathrm{WZ\,eff}}^{\mathrm{ZB\,ref}} \,. \tag{1}$$

Here, $P_{\mathrm{WZ\,eff}}^{\mathrm{ZB\,ref}}$ is the effective spontaneous polarization constant of WZ referenced to the ZB phase [Dreyer *et al.*, Phys. Rev. X **6**, 021038 (2016)].We note that while the polarization **P** is in principle a vector, we focus here on its component in the direction of the polar axis (i.e., [0001] for WZ and [111] for ZB). For ZnO, $P_{\mathrm{f}}^{\mathrm{ZB}}$=0.5 e/uc. This is also equal to the quantity $-q_{\mathrm{t}}$, if no breakdown occurs.

The effective polarization can also be defined with respect to a centrosymmetric reference system, as discussed by Dreyer *et al.*[Phys. Rev. X **6**, 021038 (2016)]. The hexagonal (H) phase, for which the formal polarization is zero, is such a reference. With respect to this reference the effective polarization of WZ is:

$$P_{\mathrm{WZ\,eff}}^{\mathrm{H\,ref}} = P_{\mathrm{f}}^{\mathrm{WZ}} - P_{\mathrm{f}}^{\mathrm{H}} \,. \tag{2}$$

Therefore, for ZnO, since $P_{\mathrm{f}}^{\mathrm{H}}$=0 and $P_{\mathrm{f}}^{\mathrm{ZB}}$=0.5 e/uc:

$$q_{\mathrm{P}} = P_{\mathrm{WZ\,eff}}^{\mathrm{ZB}} = P_{\mathrm{WZ\,eff}}^{\mathrm{H}} - 0.5e/\mathrm{uc} \,. \tag{3}$$

B. Adjusting the charge of the pseudohydrogen atom

Our proposed passivation scheme requires using psH pseudopotentials with a non-integer fractional charge. This applies to both the nuclear and the valence charge, since a pseudo-atom is a neutral object. The amount of charge by which the pseudohydrogen valence needs to be adjusted is determined by the magnitude of the polarization charge (e.g., $\mathrm{psH}^{*}_{0.5+q_{\mathrm{p}}/e}$). When using the VASP code, as done in this work, the pseudopotential with non-integer fractional valence is obtained by adjusting the valence flag ("ZVAL") in the pseudopotential

file ("POTCAR"). For example, in order to construct the $psH^{*}_{0.48}$ pseudopotential used to passivate the O dbs on the ZnO(000$\bar{1}$) surface, we set the ZVAL value in the $psH_{0.5}$ pseudopotential file (i.e., the POTCAR file in the H.5 folder of the VASP POTCAR library) to 0.48. Similarly, in the Quantum Espresso code, the charge of the pseudopotential can be modified by editing the valence flag ("z_valence"). We note, however, that not all pseudopotentials used with the Quantum Espresso code are well tested and some may exhibit a wrong alignment, even if the charges are correctly modified.

C. Energy convergence for wurtzite gallium- and aluminium-nitrides

In the main text we propose a passivation scheme for materials exhibiting spontaneous polarization, which improves the convergence behavior of slab calculations by correctly reproducing the limit of an infinitely thick slab. Here, we present additional results for other wurtzite systems, i.e. GaN and AlN, which confirm the effectiveness of the proposed scheme for materials beyond the ZnO case discussed in the main text. All results presented for GaN and AlN are calculated using PBE as exchange-correlation functional.

Supplementary Figure 2 is equivalent to Figure 1a in the main text, but shows results for AlN and GaN slabs. As such, it presents the energy difference between two wurtzite (WZ) (0001) reconstructions [(2×2)-anion$_{\mathrm{ad}}$ and (2×2)-V_{cation}] that satisfy the electron-counting (EC) rule, plotted as a function of the slab thickness. Similar to the ZnO case, the results imply that when the conventional scheme is used the energy is well converged already for relatively thin slabs in which breakdown has not yet occurred (green line). However, after breakdown occurs (blue line), a kink is observed in the curve followed by a slow convergence of the energy. In contrast, when our proposed passivation scheme is used the values converge quickly.

D. Convergence of structural properties for wurtzite aluminium-nitride

In addition to the convergence in energies, we also investigate the impact the passivation schemes have on the convergence of structural parameters. To this end we look at the convergence of interlayer spacing perpendicular to the surface of AlN slabs of increasing thickness for surfaces terminated by different surface structures, specifically the (1×1)-

clean, the (2×2)-N_{ad} and the (2×2)-V_{Al} structures. We focus on the three Al (N) layers closest to the surface and label them 1 through 3, with the outermost layer (the one closest to the surface) being 1. For each of these layers, we measure the distance, Δd, between the plane of Al(N) atoms and its neighboring plane of Al(N) atoms away from the surface. The obtained Δd values are plotted in Supplementary Figure 3 as a function of $1/d^2_{\mathrm{slab}}$.

Again we observe that rapid convergence is attained when the proposed passivation scheme is used. For this case, the interlayer distance is converged to within 0.0006 Å already for the thinnest slab (5 BLs). In contrast, the results obtained with the conventional scheme show a slow convergence.

E. Convergence of the electronic structure for wurtzite aluminium-nitride

In this section we focus on the convergence of the electronic structure with slab thickness. In Supplementary Figure 4, the total and the layer-resolved densities of states, as well as the electrostatic potential energy profiles, are shown for the AlN(2×2)-N_{ad} structure for two slab thicknesses (5 BLs and 7 BLs) and the different passivation schemes. When the conventional scheme is used (Supplementary Figures. 4a and b), the presence of an electric field in the slab leads to a shift in the bands from one layer to the next. Breakdown occurs in the 7-BL slab seen in Supplementary Figure 4b, resulting in a surface electronic structure which is different from the one of the 5-BL case. In contrast, when the proposed passivation scheme is applied (Supplementary Figures. 4c and d) the calculated densities of states remain unchanged for different slab thicknesses and the surface states due to the N_{ad} can be unambiguously identified.

Similar differences are observed in the surface band structure, as seen in Supplementary Figure 5. The shown surface band structures are for the AlN(1×1) clean surface and the AlN(2×2)-N_{ad} reconstruction and slabs with a thickness of 9 BL. Since breakdown occurs in the 9-BL slab when the conventional passivation scheme is used, the conduction band at the backside of the slab becomes occupied (near 0 eV), as shown in Supplementary Figures. 5a and b. When the proposed passivation scheme is applied (Supplementary Figures 5c and d) a distinct band gap is seen and the surface states related to the reconstructed surface become visible: a partially filled Al dangling bond in Supplementary Figure 5c and a partially filled N_{ad} dangling bond in Supplementary Figure 5d.

F. Convergence using the HSE06 functional for wurtzite zinc-oxide

It was mentioned in the *Computational details* section of the main text that we use the PBE functional to study the energetics and the HSE06 functional to study the electronic structure. This choice was made because tests we performed revealed that energies are extremely difficult to converge using HSE06, regardless of the passivation scheme. Details of these tests are discussed her.

We analyze the energy difference ΔE between two WZ ZnO(0001) electron-counting reconstructions [(2×2)-O_{ad} and (2×2)-V_{Zn}] as a function of different variables including the vacuum thickness, the slab thickness, the cutoff energy, and the mixing parameter α (the fraction of Hartree-Fock exchange that is mixed with PBE exchange in HSE06). The results are shown in Supplementary Figure 6.

In Supplementary Figure 6a, the energy difference is plotted as a function of $1/d_{\mathrm{slab}}$ (where d_{slab} is the slab thickness), for values of the mixing parameter ranging from 0 % (i.e., pure PBE) to 36 %. For PBE (blue solid and dashed lines) we observe a slow convergence when using the conventional passivation scheme and fast convergence when using the proposed scheme, as reported in the main text. A very different convergence behavior is seen for the hybrid functional.

Previous studies [Horowitz *et al.*, Phys. Rev. Lett. **97**, 026802 (2006); Engel, J. Chem, Phys. **140**, 18A505 (2014); Engel, Phys. Rev. B **97**, 075102 (2018)]shed light on this behavior and related it to the asymptotic behavior of exact exchange (EXX), which is proportional to $1/z$, with z being the distance from the surface into the vacuum region. This slow decay of the EXX energy affects the convergence of the DFT total energy calculated using the HSE06 functional. In Supplementary Figure 6b, the same quantity, ΔE, is plotted as a function of $1/d_{\mathrm{vac}}$, where d_{vac} is the vacuum thickness (ranging from 14 Å to 36 Å), for a slab thickness fixed to 5 BL and a slab passivated on one side using the conventional scheme. We can see that the energy values are easily converged in PBE: an accuracy of 1 meV/uc is reached already at 14 Å vacuum thickness. In contrast, convergence is poor for HSE06.

In Supplementary Figure 6c we examine the possible impact of the cutoff energy by plotting ΔE calculated using HSE06 as a function of $1/d_{\mathrm{slab}}$ and cutoff energies ranging from 500 eV to 800 eV. We find that 500 eV, commonly considered to be a sufficient high cutoff

energy to obtain converged results with PBE, is not sufficient to obtain converged results with HSE06. Engel [J. Chem. Phys. **140**, 18A5050 (2014)] reported that an extremely large cutoff energy of 2000 Ry (roughly 27200 eV) is necessary to show a clean asymptotic decay of the $2s$ orbital of atomic carbon.

These results lead us to the conclusion that an extremely thick vacuum region and very large cutoff energies are required to be able to analyze energy convergence to an accuracy of a few meV when the HSE06 functional is used. For this reason we decided to use the PBE functional to analyze the impact of our proposed passivation scheme on the convergence behavior of energies.

II. SUPPLEMENTARY FIGURES

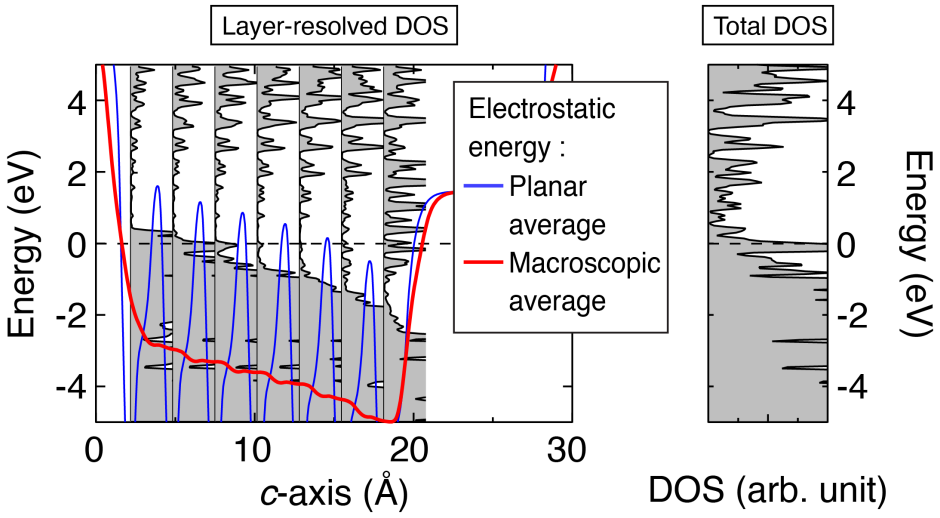

Supplementary Figure 1. **Electrostatic potential energy profile and LDOS.** ZB ZnO(111) (1×1) 7 BL slab to which no passivation is applied and breakdown has occurred, i.e., charge has been transferred from one side of the slab to the other. The planar-averaged and the macroscopic electrostatic potential energies are shown as blue and red solid lines, respectively. The LDOS along the z-axis (axis perpendicular to the slab surfaces) is resolved for each Zn-O BL and shown in grey. The energy of the highest occupied state is set to 0 eV.

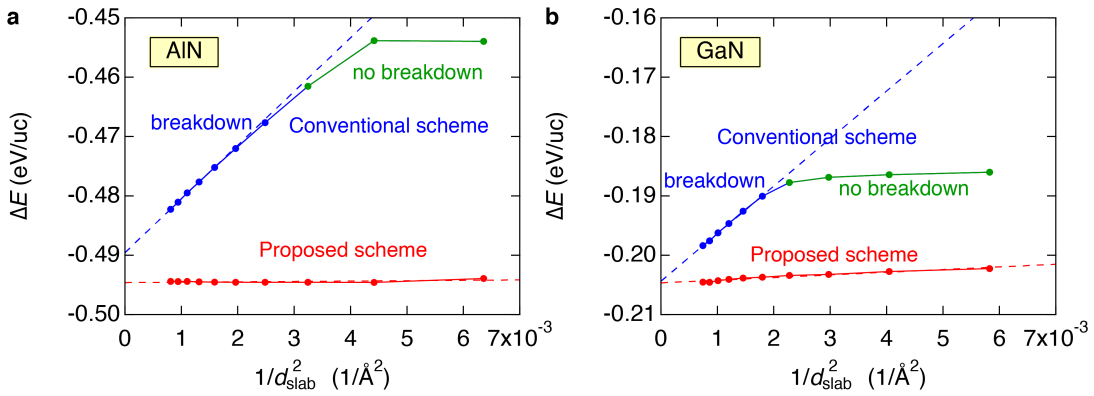

Supplementary Figure 2. **Convergence of passivation schemes as a function of slab thickness.** The energy difference between two WZ (0001) reconstructions [(2×2)-anion$_{\mathrm{ad}}$ and (2×2)-V$_{\mathrm{cation}}$] as a function of $1/d^2_{\mathrm{slab}}$, where d_{slab} is the thickness of an **a** AlN and **b** GaN slab. Red solid lines show results calculated using the proposed passivation scheme. Results obtained using the conventional scheme are depicted by green solid lines for the system before the occurrence of breakdown and blue solid lines for the system after breakdown. The dashed lines show the extrapolated value for an infinitely thick slab.

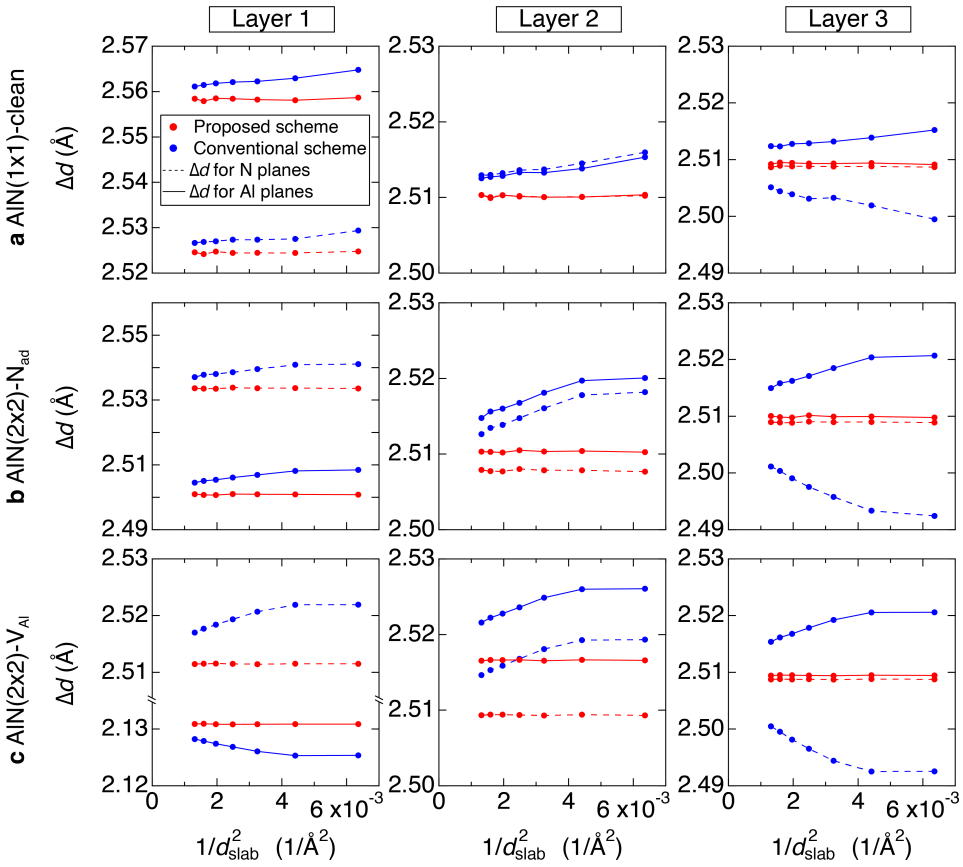

Supplementary Figure 3. **Convergence of the interlayer spacing at the surface as a function of $1/d^2_{\mathrm{slab}}$, where d_{slab} is the thickness of the considered AlN(0001) slab.** Considered are slabs with a **a** AlN(1×1)-clean, **b** AlN(2×2)-$\mathrm{N_{ad}}$ and **c** AlN(2×2)-$\mathrm{V_{Al}}$ surface termination. Red and blue lines represent Δd values obtained by using the proposed and the conventional passivation scheme, respectively. Solid (dashed) lines depict Δd values for the Al (N) planes.

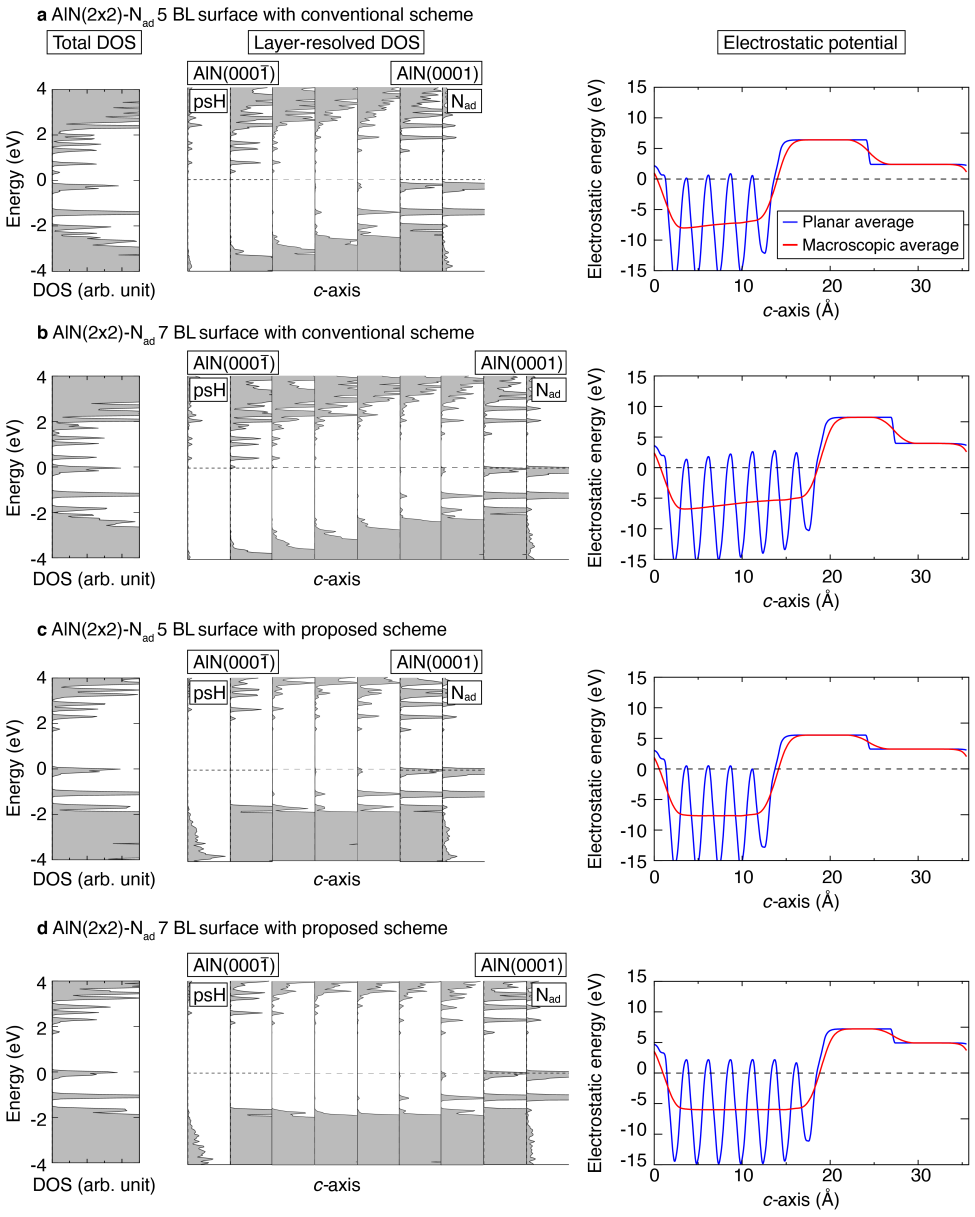

Supplementary Figure 4. **The calculated total and layer-resolved density of states, and the electrostatic potential energy profile for AlN(0001) slabs of varying thicknesses and using different passivation schemes.** Shown are AlN **a** 5 BL and **b** 7 BL slabs with db saturated using the conventional passivation, and **c** 5 BL and **d** 7 BL using the proposed passivation schemes. A AlN(2×2)-N_{ad} reconstruction is used for the Al-terminated surface. The planar and the macroscopic averaged electrostatic potential energies are shown as blue and red solid lines in plot of the electrostatic potential energy profiles. The layer-resolved DOS is shown along the z-axis (axis perpendicular to the slab surfaces) as a grey region for each Al-N BL.

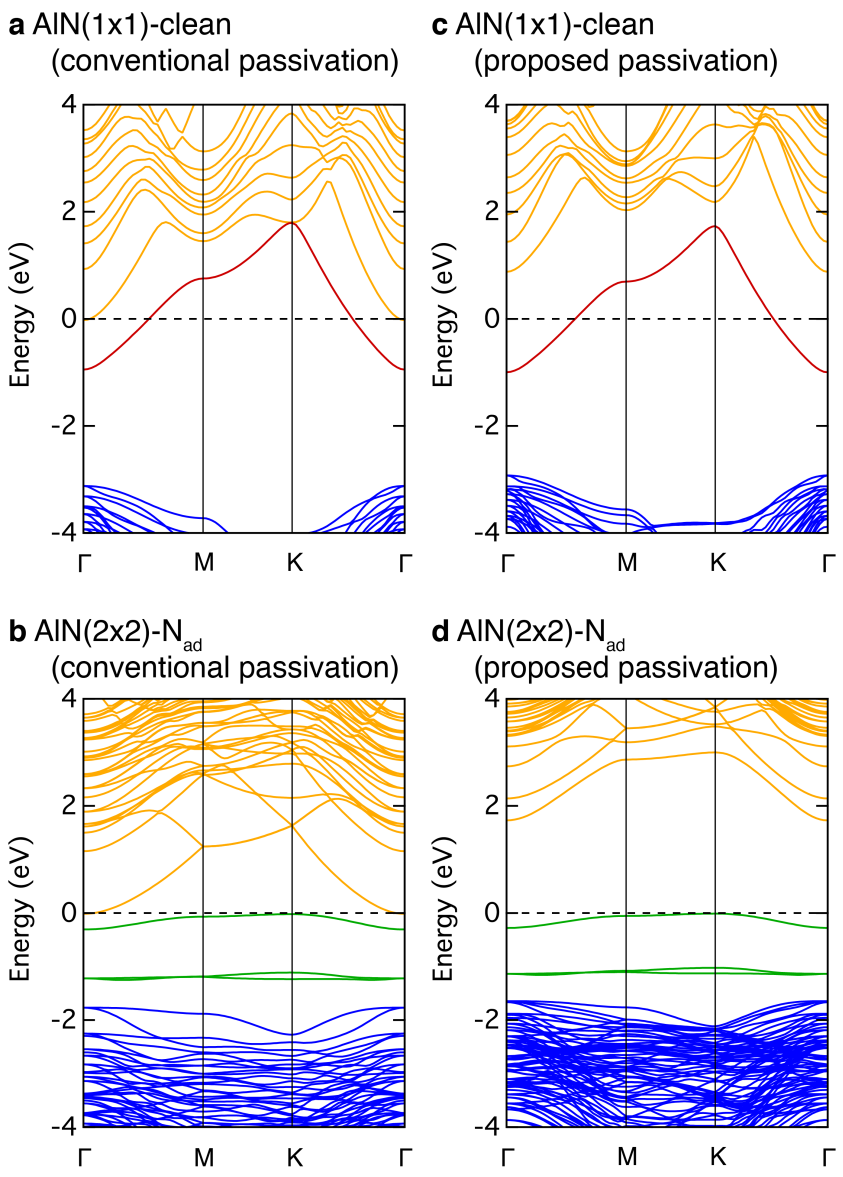

Supplementary Figure 5. **Band structures calculated for different AlN(0001) surface structures.** **a**, **c** (1×1) clean surface and **b**, **d** (2×2)-N_{ad} reconstructions, both calculated using a 9 BL slab. **a** and **b** show results obtained by applying the conventional passivation scheme to the back side of slab, while **c** and **d** show results obtained using the proposed passivation scheme. The energy of the highest occupied state is set to 0 eV. Conduction bands are shown in yellow, valence bands in blue. The partially occupied surface state on the clean surface is shown in red, while the fully occupied surface states on the reconstructed surface are shown in green.

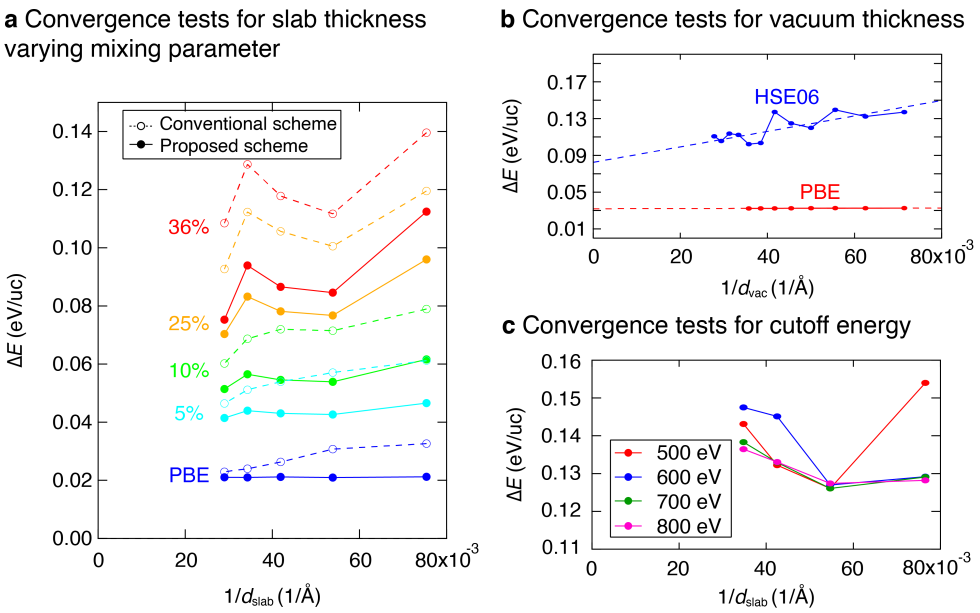

Supplementary Figure 6. **Tests for the convergence of energy with slab thickness using PBE and HSE06 as exchange-correlation functionals.** **a** Dependence of the calculated energy difference ΔE between two ZnO(0001) reconstructions [(2×2)-O_{ad} and (2×2)-V_{Zn}] on $1/d_{slab}$, where d_{slab} is the slab thickness. Results are shown for different values of the mixing parameter α in the HSE06 functional. α values are written next to each line with the corresponding color in a unit of %. Solid and dashed lines indicate values obtained using the proposed and the conventional passivation schemes, respectively. **b** The energy difference ΔE as a function of $1/d_{vac}$, where d_{vac} is the thickness of vacuum region within the supercell. Red and blue solid lines indicate results calculated using PBE and HSE06 ($\alpha = 25\,\%$), respectively. Dashed lines show the extrapolation to an infinitely thick vacuum region. **c** The energy difference ΔE dependence on $1/d_{slab}$, for values of the cutoff energy ranging from 500 eV to 800 eV. In both (b) and (c), the backside of the slab is passivated using the conventional scheme.